Accepted Manuscript

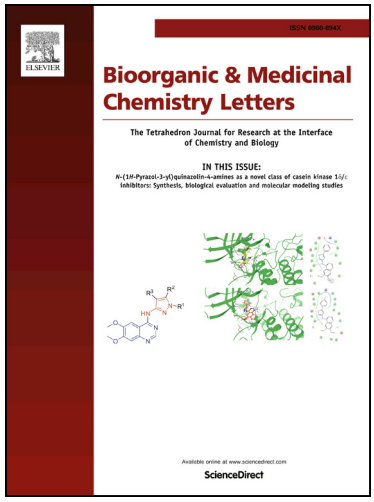

A New Chemotype Inhibitor for the Human Organic Cation Transporter 3 (hOCT3)

Xiaolei Pan, Kavita A. Iyer, Hebing Liu, Douglas H. Sweet, Małgorzata Dukat

PII: S0960-894X(17)30796-5
DOI: http://dx.doi.org/10.1016/j.bmcl.2017.08.008
Reference: BMCL 25202

To appear in: *Bioorganic & Medicinal Chemistry Letters*

Received Date: 29 June 2017
Revised Date: 3 August 2017
Accepted Date: 4 August 2017

Please cite this article as: Pan, X., Iyer, K.A., Liu, H., Sweet, D.H., Dukat, M., A New Chemotype Inhibitor for the Human Organic Cation Transporter 3 (hOCT3), *Bioorganic & Medicinal Chemistry Letters* (2017), doi: http://dx.doi.org/10.1016/j.bmcl.2017.08.008

A New Chemotype Inhibitor for the Human Organic Cation Transporter 3 (hOCT3)

Xiaolei Pan,[a♦] Kavita A. Iyer,[b♦] Hebing Liu,[a] Douglas H. Sweet,[a] Małgorzata Dukat[b*]

[a]*Department of Pharmaceutics,* [b]*Department of Medicinal Chemistry, School of Pharmacy, Virginia Commonwealth University, Richmond, VA 23298, USA*

♦Co-first authors

*Corresponding author. Tel.: 8048285256; fax: 8048287625.

E-mail address: mdukat@vcu.edu (M. Dukat)

Address: Department of Medicinal Chemistry, School of Pharmacy, Virginia Commonwealth University, PO Box 980540, Richmond, VA 23298-540, USA

BMCL_ August 3_2017_revised

ABSTRACT

Human organic cation transporters (OCTs) represent an understudied neurotransmitter uptake mechanism for which no selective agents have yet been identified. Several neurotransmitters (e.g. serotonin, norepinephrine) are low-affinity substrates for these transporters, but possess higher affinity for other transporters (e.g. the serotonin or norepinephrine transporters; SERT and NET, respectively). We have identified a new class of OCT inhibitors with a phenylguanidine structural scaffold. Here, we examine the actions of a series of such compounds and report preliminary structure-activity relationships (SARs) – the first dedicated SAR study of OCT3 action. Initial results showed that the presence of a substituent on the phenyl ring, as well as its position, contributes to the phenylguanidines' inhibitory potency (IC_{50} values ranging from 2.2 to >450 μM) at hOCT3. There is a trend towards enhanced inhibitory potency of phenylguanidines with increased lipophilic character and the size of the substituent at the phenyl 4-position, with the latter reaching a ceiling effect. The first PiPT-based hOCT3 homology models were generated and are in agreement with our biological data.

KEY WORDS

OCT3, phenylguanidines, 3D homology model, in vitro studies, SAR

Organic cation transporters (OCTs) represent a family of transport proteins for which few, if any, specific agents are available. That is, most agents that serve as substrates or inhibitors at OCTs have other primary targets (i.e., receptors or other transporters). Antidepressants are a case in point. Although inhibitors of OCTs in the μM range,[1] many antidepressants bind at, for example, the serotonin transporter in the low nM range. Hence, there is a need for new agents to better investigate OCT-specific functions. A diverse array of pharmacologically-relevant xenobiotics, drugs, model cations, and endogenous ligands (e.g., aminergic neurotransmitters), are targets for organic cation transporters.[2,3] Currently, three major human OCT paralogs: OCT1, OCT2, and OCT3 (SLC22A1, 2 and 3, respectively), have been well characterized as polyspecific, electrogenic, and Na^+/Cl^--independent uniporters.[4,5] In the CNS, OCTs appear to function as low-affinity, high-capacity uptake-2 transporters, opposite to, for example, the high-affinity, low-capacity 5-HT, DA, and NE transporters (uptake-1) (i.e., SERT, DAT, NET, respectively).[6,7] OCT1 is found primarily in the liver,[8] OCT2, in addition to its major expression in kidney, exists in the brain,[8,9] whereas OCT3 is expressed primarily in the brain[10] and is found in other organs (i.e., heart, liver, kidney, lung, intestine, placenta and adrenal gland).[11,12] In the brain, non-neuronal uptake through OCTs expressed in glia and glial cells exceeds that by neurons by ~10-fold, suggesting that OCTs are also important regulators of brain monoamines.[13] Because OCTs are complementary and/or an alternative clearance pathway to 5-HT, DA, and NE transporters they are promising therapeutic targets for a variety of neuropsychiatric disorders associated with the imbalance of synaptic concentrations of aminergic neurotransmitters.[14]

The polyspecific character of OCTs makes them a significant target for structurally diverse molecules and, so far, systematic structure-activity relationship (SAR) studies are lacking. Guanidine is a weak inhibitor of OCT3 (IC_{50} = 2200 – 6200 μM).[15] However, certain substituted

guanidines are more potent.[16,17] In an investigation of 5-HT_3 receptor ligands, we developed a series of phenylguanidines that we then examined for interaction at the OCTs.[18] One of the compounds, 3-chlorophenylguanidine (3-CPG; **1**) was found to be a much (nearly 1000-fold) more potent inhibitor at hOCT3 than guanidine itself. Here, we report on preliminary SAR for hOCT3 inhibitors containing a phenylguanidine scaffold. Inhibition was measured as uptake of a known substrate, [^{3}H]MPP^+, in the presence and absence of the phenylguanidines using HEK293 cells stably-expressing hOCTs. To understand the interactions of substituted phenylguanidines in the binding region we generated the first inorganic phosphate transporter (PiPT)-based hOCT3 model. This investigation also represents the first dedicated SAR study to examine OCT3 transporters.

3-Chlorophenylguanidine nitrate (3-CPG; **1**) was on hand from a previous project.[19,20] Phenylguanidines **2-6** were re-synthesized for these studies using the general method depicted in Scheme 1, previously published by us.[20,21] Phenylguanidines **7**-**9** are new and were prepared in a similar manner as analogs **2**-**6** (Scheme 1; see Supplementary material for experimental details). In short, commercially available, appropriately-substituted anilines were converted to their corresponding hydrochloride salts and then reacted with cyanamide in a condensation reaction to give the desired guanidines as hydrochloride salts. The targets, **2**-**9**, were obtained as nitrate salts by treating the phenylguanidine hydrochlorides with an excess of ammonium nitrate followed by recrystallizations from ethanol. We have found that nitrate salts of phenylguanidines are much less hygroscopic than their hydrochloride salts.

Scheme 1. Synthetic pathway for phenylguanidines **2-9**.

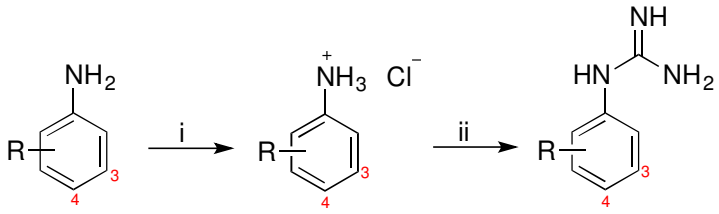

R = H,
4-Cl,
4-CH_3,
4-*t*Bu,
4-Bn,
4-F,
4-Br,
4-I

R = H (**2**),
4-Cl (**3**),
4-CH_3 (**4**),
4-*t*Bu (**5**),
4-Bn (**6**),
4-F (**7**),
4-Br (**8**),
4-I (**9**)

[a]Reagents and conditions: (i) HCl, EtOH; (ii) (a) NH_2CN, EtOH, reflux; (b) NH_4NO_3, H_2O.

The structures of **2**-**6** were confirmed by ^{1}H NMR, IR and mp and are consistent with that reported in the literature.[19-21] Since **7**-**9** were unknown, their structures were additionally confirmed by instrumental methods and elemental analysis.

MPP$^+$ concentration and uptake time used for kinetic analyses were determined previously.[22,23] The K_m value for MPP$^+$ at hOCT3 was 32.1 µM, comparable to the value reported in the literature.[10] Inhibition of hOCT-mediated [^{3}H]MPP$^+$ accumulation was quantified in the presence of increasing concentrations (1x10^{-8} to 1x10$^{-2.5}$ M) of unlabeled phenylguanidines (see Supplementary material for experimental details). 3-Chlorophenylguanidine (3-CPG; **1**) produced marked inhibition of hOCT3 transport activity (IC_{50} = 7.6 µM; Figure 1, Table 1). The presence and/or position of the Cl group might be important for the inhibitory actions of **1** at hOCT3. Thus, to better understand the role of the Cl group we prepared deschloro analog **2** (PG) and a positional isomer of **1**, 4-chlorophenylguanidine (4-CPG; **3**). Removal of the Cl group resulted in a

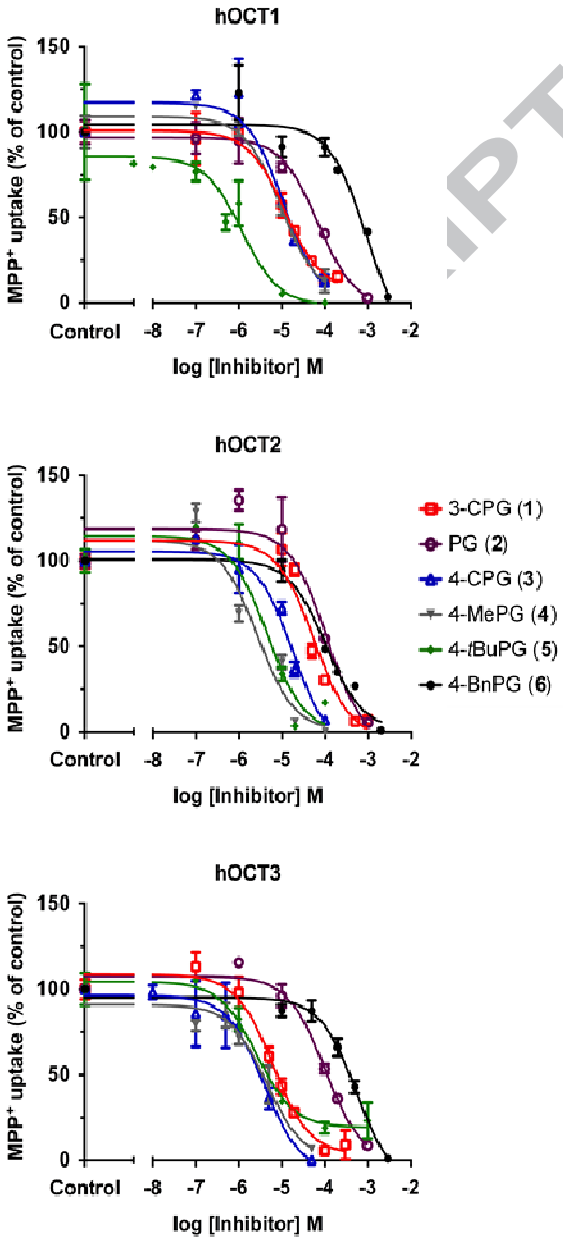

Figure 1. Inhibitory potency determination. Representative experiments showing 1 min uptake of MPP$^+$ (1 µM) measured in HEK293 cells stably expressing hOCTs in the presence of increasing concentrations of phenylguanidine analogs (10^{-8} to 10$^{-2.5}$ M). Data were corrected for nonspecific background measured in empty vector control cells and are shown as mean ± SD. IC_{50} values were determined with nonlinear regression and are reported in Table 1.

13-fold decrease in potency (**2**, IC_{50} = 99.8 μM) indicating that the presence of the Cl group contributes to inhibitory activity at hOCT3.Translocation of the 3-Cl group to the 4-position of the phenyl ring, as seen in **3** (IC_{50} = 2.8 μM), slightly increased inhibitory potency (Table 1).

The observed inhibitory effect of **3** could be due to the electronic or lipophilic character of the Cl group. To assess this we synthesized the 4-CH_3 analog **4** (4-MePG). The CH_3 and Cl groups possess similar lipophilic properties (π = 0.56 and 0.71, respectively) but opposite electronic properties (σ = -0.17 and 0.23, respectively).[24] Thus, if the observed inhibitory effects were due to the lipophilic property, π, of the Cl group, 4-MePG (**4**) should be about as potent as 4-CPG (**3**). However, if the electronic, σ, property is important, 4-MePG (**4**) would be expected to be less potent than **3** or inactive as an inhibitor. Phenylguanidine **4** (IC_{50} = 4.6 μM) was found to be nearly equipotent to analog **3** (Figure 1, Table 1) indicating that lipophilic character of the substituent likely contributes to the inhibitory activity of phenylguanidines at hOCT3. Replacement of the 4-CH_3 substituent with a more lipophilic *t*Bu (π = 1.98)[24] group resulted in a 2-fold increase in inhibitory potency as seen for 4-*t*BuPG (**5**; Figure 1, Table 1).

However, lipophilicity isn't the only parameter contributing to the inhibitory potency of phenylguanidines because 4-benzylphenylguanidine (4-BnPG; **6**) (IC_{50} = 452.5 μM) was >200-fold less potent as an inhibitor of hOCT3 (Figure 1, Table 1) than **5** despite its comparable lipophilic character (π = 1.79).[24] The dramatic decrease in inhibitory activity of **6** might be related to the significant increase in the steric bulk of the benzyl (Bn) group compared to *t*Bu in **5**. It appears that inhibitory activity increases with an increase in the size of the substituent, i.e. from H to CH_3 to *t*Bu, and then reaches an upper limit (ceiling effect). Thus, the weak inhibitory

activity of **6** for hOCT3 might be related to the introduction of the aromatic ring present in the Bn group or bulk intolerance associated with the binding region as discussed in the molecular modeling section below.

Further, to investigate the steric properties at the 4-position, we synthesized and tested other 4-halo-subsituted analogs (4-F, 4-Br and 4-I). Both the 4-Br (IC_{50} = 4.8 μM) and the comparatively larger 4-I (IC_{50} = 1.8 μM) substituted phenylguanidine analogs retained comparable inhibitory potency at hOCT3 (Table 1, Figure S1) and agreed with the increased lipophilicity requirement for potency observation. The compound with the substantially less lipophilic and smaller 4-F (π = 0.14)[24] group was ~10-fold less potent than 4-CPG (**3**; Table 1).

Table 1. Inhibitory potencies (IC_{50} ± SEM μM) of phenylguanidine analogs **1-9** at hOCT1-3.

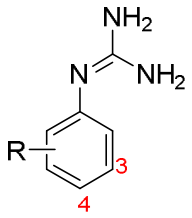

Compound	R	IC_{50}[a] ± SEM (μM) hOCT1	hOCT2	hOCT3
1 (3-CPG)	3-Cl	13.7 ± 0.8	60.5 ± 4.1	7.6 ± 0.7
2 (PG)	H	41.1 ± 14.4	89.0 ± 12.2	99.8 ± 2.8
3 (4-CPG)	4-Cl	10.0 ± 0.6	18.9 ± 0.1	2.8 ± 0.7
4 (4-MePG)	4-CH_3	10.0 ± 0.2	9.3 ± 4.8	4.6 ± 1.1
5 (4-*t*BuPG)	4-*t*Bu	0.9 ± 0.2	8.3 ± 3.9	2.2 ± 0.2
6 (4-BnPG)	4-CH_2Ø	761.9 ± 254.7	96.2 ± 8.0	452.5 ± 87.9
7 (4-FPG)	4-F	22.6 ± 0.8	48.3 ± 18.9	27.8 ± 11.0
8 (4-BrPG)	4-Br	6.3 ± 1.0	11.3 ± 3.2	4.8 ± 0.7
9 (4-IPG)	4-I	2.4 ± 0.3	4.4 ± 1.5	1.5 ± 0.3

[a]Values presented as the mean ± SEM (n = 3)

We also examined phenylguanidines **1**-**9** for subtype selectivity at hOCT3 vs hOCT2 vs hOCT1 and found that they also inhibit MPP^+ uptake at hOCT1 and hOCT2. A slight paralog selectivity (less than 10-fold) was seen for the Cl-substituted analogs (Table 1). That is, 3-CPG (**1**) and 4-CPG (**3**) showed 8- and 6-fold selectivity for hOCT3 vs hOCT2. Other phenylguanidines displayed very modest selectivity (less than 5-fold) among all three hOCT paralogs (Table 1).

To understand inhibition of hOCT3 by the phenylguanidines and their interactions at the atomic level (modeling studies) their mode of inhibition was determined. Saturation analysis was performed for hOCT3 in the absence and presence of two different concentrations of phenylguanidine **3** or **5** (Figure 2). Using nonlinear regression analysis of background-corrected data, substrate uptake curves were fit to the equation for mixed-model inhibition, and α

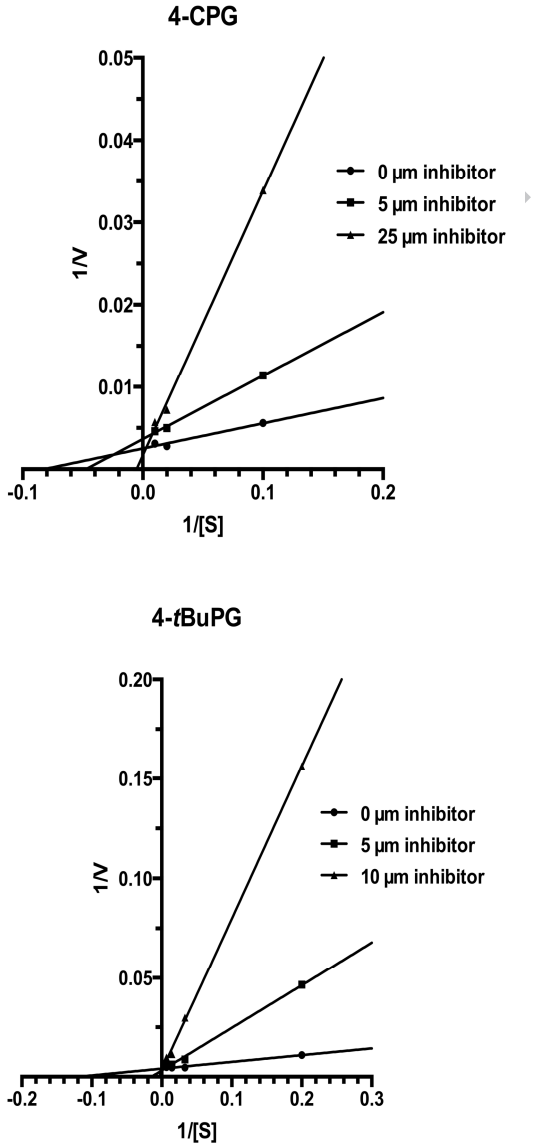

Figure 2. Competitive inhibition of hOCT3-mediated phenylguanidine transport. One minute cellular accumulation assays were conducted for MPP^+ (1-150 µM) in the presence and absence of two concentrations of either 4-CPG (**3**) or 4-*t*BuPG (**5**) as indicated. After correction for non-hOCT3 mediated background accumulation of MPP^+ in non-transporter expressing control cells, saturation curves were generated and analyzed by nonlinear regression to determine the mode of inhibition. Lineweaver-Burk transformations of the data are shown to readily allow visualization of the mode of inhibition as competitive.

values were calculated for each analog. The estimated α values for **3** and **5** were greater than 1 (i.e., α = 23 and 17.5, respectively), indicating that these phenylguanidines are competitive inhibitors of hOCT3. To readily visualize the data Lineweaver-Burk plots were constructed (Figure 2) clearly showing increasing K_m (changing x-intercept), but unaltered V_{max} (consistent y-intercept) in the presence of inhibitor. We also examined the mode of inhibition for a standard inhibitor of OCTs, quinine, and found that it also behaved as competitive inhibitor of hOCT3 (α = 3.9; data not shown).

In 2013, the crystal structure of the inorganic phosphate transporter (PiPT; PDB ID: 4J05) in complex with a phosphate molecule was solved by Pedersen et al.[25] PiPT belongs to the phosphate:H^+ symporter family in the major facilitator superfamily[26] and shares homology with members of the SLC22 transporter family.[27-29] As such, PiPT was used as a template for homology modeling of these transporters until their crystal structures are solved since it was argued that "human members of the SLC22, SLC15, and SLC2 families adopt the MFS (major facilitator superfamily) fold, despite not sharing significant sequence similarity among them"[30] thereby indicating an overall similar 3-D arrangement. While our modeling studies were underway, in 2017, Dakal et al.[31] published models of hOCT1-3 among others based on the crystal structure of human glucose transporter (GLUT3; PDB ID: 5C65) belonging to the SLC2A3 family of transporters as the template. The resolution of the GLUT3 crystal structure at 2.65 Å[32] is only slightly better than that of our template, PiPT at 2.9 Å.[25] Moreover, the sequence identity between GLUT3 and hOCT3 appears to be ~20% which is no better than the sequence identity between PiPT and hOCT3 (~23%). Dakal et al.[31] mentioned considering the PiPT crystal structure as a potential template but summarily rejected it in favor of GLUT3. The

only results of validation that Dakal et al.[31] provide for their models are Ramachandran plots. The authors neglected to dock the known substrate, MPP^+, in any of their models. As such, at the given time, models based on PiPT or GLUT3 are equally plausible.

Both the template, PiPT, and the protein of interest, hOCT3, consist of 12 transmembrane-spanning helices with intracellular N- and C-termini.[25,27] The binding region of organic cation transporters has been defined as a fairly large region composed of smaller overlapping binding sites.[33] The amino acid residues Trp218, Tyr222, and Thr226 (TMD 4), Ala443, Leu447 and Gln448 (TMD 10) and Asp475 (TMD 11) have been proposed to comprise the binding region in rOCT1.[33,34] The model substrate MPP^+ has been shown to interact with these residues.

Mutagenesis data implicate Asp475 in rOCT1 to be a critical amino acid residue for interactions of MPP^+ at the transporter since the mutation Asp475Glu led to a 94% decrease in the V_{max} of MPP^+ uptake.[33,34] Therefore, we used the corresponding amino acid residue in hOCT3, i.e. Asp478, to define the binding site. Upon docking (see Supplementary material for experimental details), the protonated nitrogen atom of MPP^+ was seen to be involved in ionic salt-bridge interactions with the carboxylate oxygen atom of Asp478 (Figure S2). Additionally, the protonated nitrogen atom formed a cation–π interaction with the aromatic ring of Trp223. The pyridine ring of MPP^+ was involved in a T-shaped π–π stacking interaction with Phe165 (Figure S2). The guanidinium moiety of the side chain of Arg20 formed a cation–π interaction with the aromatic ring of MPP^+ that is further involved in hydrophobic interactions with Leu23 and Tyr365 (Figure S2).

Our kinetics studies indicated that 4-CPG (**3**) and 4-*t*BuPG (**5**) are competitive inhibitors (see Figure 2) at hOCT3. Therefore, we docked the phenylguanidine analogs at the substrate binding region of hOCT3 using Asp478 to define it. We obtained two different docking modes for phenylguanidines **1**-**9** referred to as mode 1 and mode 2 as shown in 'Supplementary material', Figures S3 and S4, respectively.

In mode 1, all phenylguanidines except 4-BnPG (**6**) docked in a similar and overlapping manner with the guanidinium moiety directed towards Asp478 (Figure 3 and Figure S3). 4-BnPG (**6**), on the other hand, was flipped over with the guanidinium moiety directed at the other end of the binding region towards Glu451 (Figure 3 and Figure S3). In contrast, in mode 2, all nine phenylguanidines, including 4-BnPG (**6**) docked in an overlapping manner and formed ionic salt-bridge interactions with the carboxylate oxygen of Asp478 (Figure 4 and Figure S4).

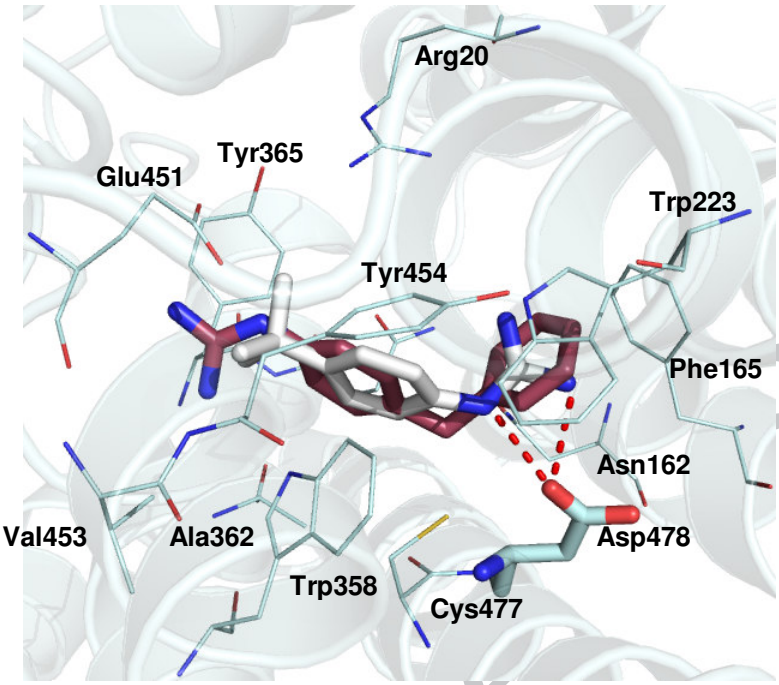

Figure 3. Docking mode 1 of phenylguanidines with 4-*t*BuPG (**5**; white) and 4-BnPG (**6**; raspberry) superimposed at the binding region of hOCT3. The amino acid residues of hOCT3 are displayed as pale cyan lines. Dashed red lines represent ionic salt bridge interactions between the N atoms of the guanidine moiety of 4-*t*BuPG (**5**; white) and the carboxylate oxygen of Asp478 (pale cyan-capped sticks). The 4-BnPG analog is flipped over so that the guanidine moiety is pointing towards Glu451 present on the other end of the binding region.

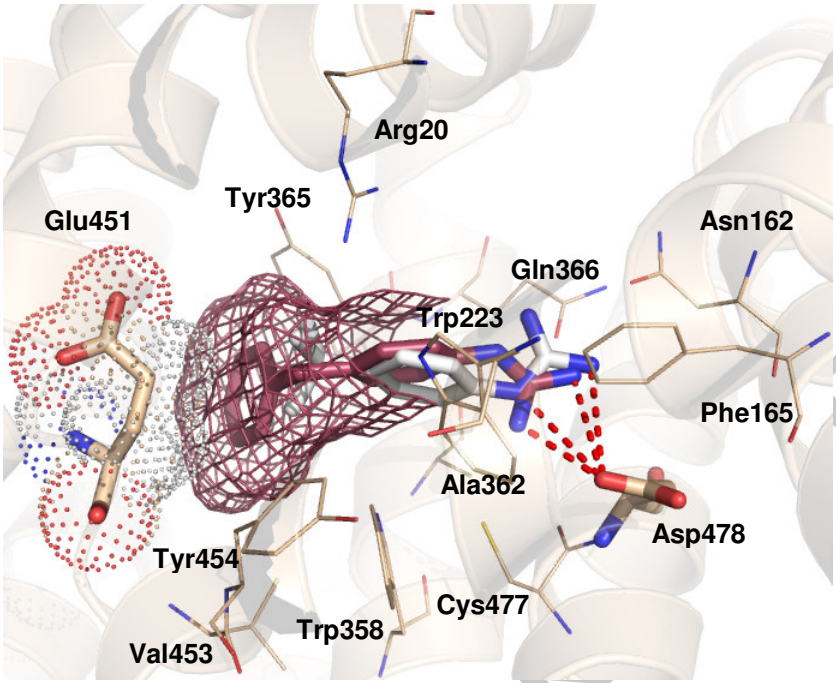

Figure 4. Docking mode 2 of 4-*t*BuPG (**5**; white) and 4-BnPG (**6**; raspberry) superimposed at the binding region of hOCT3. The amino acid residues of hOCT3 are displayed as wheat lines. Dashed red lines represent bidentate ionic salt bridge interactions between the N atoms of the guanidine moiety of phenylguanidines and the carboxylate oxygen of Asp478 (wheat-capped sticks). The 4-BnPG (**6**) analog is aligned with other phenylguanidne analogs with the guanidine moiety pointing towards Asp478. HINT analysis shows clashes between the benzyl group (meshed surface) of 4-BnPG (**6**) and Glu451 (dotted surface) present on the other end of the binding region.

To determine which of the two binding modes is more probable, we conducted a Hydropathic INTeraction (HINT) analysis[35] and compared and contrasted the interactions between the phenylguanidines and hOCT3. In general, the higher the positive HINT score, the more favorable the interactions between the two molecules. For mode 1, one of the most potent analogs, 4-*t*BuPG (**5**), and the weakest inhibitor, 4-BnPG (**6**), had negative HINT scores (Table 2). 4-BnPG (**6**) is 205–fold less potent than 4-*t*BuPG (**5**) (Table 1). For mode 2, all analogs, except 4-BnPG (**6**), had a positive HINT score (Table 3). Moreover, the unsubstituted PG (**2**),

which displayed 45–fold lower inhibitory potency compared to 4-*t*BuPG (**5**), showed a <5 but >1.5–fold lower HINT score than the other phenylguanidine analogs (Table 3). In mode 2, HINT analysis revealed that the benzyl group of 4-BnPG (**6**) clashes with the Glu451 residue (Figure 4) that is located at the other end of the binding region. Our biological data favor mode 2 vs mode 1.

Table 2. HINT scores for mode 1 of interactions of phenylguanidines **1**-**9** at hOCT3.

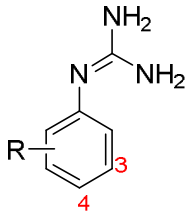

Ligands	R	HINT score	Amino acids interacting with substituents
1 (3-CPG)	3-Cl	338	Arg20, Gln247, Trp358
2 (PG)	H	549	-
3 (4-CPG)	4-Cl	547	Trp358, Ser361, Ala362, Tyr365
4 (4-MePG)	4-CH_3	356	Ala362, Tyr365
5 (4-*t*BuPG)	4-*t*Bu	-467	Val453, Ser361, Ala362, Tyr365
6 (4-BnPG)	4-CH_2Ø	-484	Ala362, Tyr365
7 (4-FPG)	4-F	566	Ala362
8 (4-BrPG)	4-Br	519	Ser361, Ala362, Tyr365
9 (4-IPG)	4-I	478	Ser361, Ala362, Tyr365

Table 3. HINT scores for mode 2 of interactions of phenylguanidines **1**-**9** at hOCT3.

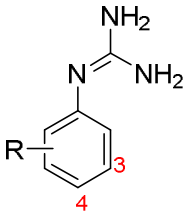

Ligands	R	HINT score	Amino acids interacting with substituents
1 (3-CPG)	3-Cl	426	Arg19, Arg20, Trp223
2 (PG)	H	96	-
3 (4-CPG)	4-Cl	250	Arg20, Trp223
4 (4-MePG)	4-CH_3	144	Trp223, Phe250
5 (4-*t*BuPG)	4-*t*Bu	143	Phe250, Tyr365, Val453, Trp358
6 (4-BnPG)	4-CH_2Ø	-7	Val453
7 (4-FPG)	4-F	222	-
8 (4-BrPG)	4-Br	252	-
9 (4-IPG)	4-I	209	Glu451

HINT analysis further indicated that the aryl substituent on the phenylguanidine moiety is involved in hydrophobic interactions at hOCT3 with residues such as Arg19, Arg20, Trp223, Phe250, Tyr365, Trp358 and Val453 (Table 3). The unsubstituted PG (**2**) is unable to participate in these hydrophobic interactions (Table 3) and this might account for its low inhibitory potency at hOCT3 (Table 1).

This is the first investigation dedicated to the SAR of hOCT3 inhibitors. Nine compounds were examined and their inhibitory potencies varied over a >200-fold range. The aryl-unsubstituted phenylguanidine **2** displayed modest potency as a hOCT3 inhibitor (IC_{50} = 99.8 μM), but introduction of a 4-Cl group enhanced potency by 35-fold. The contribution of the Cl seems to be lipophilic, rather than electronic, in nature in that it could be replaced by a methyl group (comparing **3** and **4**) with little effect on potency. The more lipophilic 4-*t*Bu analog **5** also was a potent hOCT3 inhibitor. The series of compounds examined shows that aryl substituents can influence the potency of the phenylguanidines and provides impetus for continued investigation. Due to variation in the potencies of **1**-**9** at hOCT1-3, it might ultimately be possible to develop paralog-selective compounds.

The first PiPT-based hOCT3 homology models were generated and probed with competitive inhibitors, phenylguanidines. Although, two possible modes of interactions were identified, HINT analysis coupled with biological data support mode 2.

Although yet to be optimized, a new chemotype of OCT inhibitors has been identified, phenylguanidines. The potential of these compounds is currently being exploited to develop tools to investigate these underexplored transporters.

Supplementary material

Supplementary data associated with this article can be found, in the online version, at …

Inhibitory potency determination for phenylguanidines **7**-**9** (Figure S1); MPP^+ in the binding site of hOCT3 (Figure S2); docking mode 1 of phenylguanidines **1**-**9** superimposed in the binding site of hOCT3 (Figure S3); docking mode 2 of phenylguanidines **1**-**9** superimposed in the binding site of hOCT3 (Figure S4); sequence alignment of hOCT3 and PiPT (Figure S5); Ramachandran plot (Figure S6); Experimental Section (Synthesis; Biological studies; Molecular modeling).

Author Contributions

M. D. conceived the idea, supervised the work and prepared the first draft of the manuscript; K. A. I. resynthesized known phenylguanidines and prepared several additional novel analogs, generated homology models, and conducted docking studies and HINT analysis under the supervision of M. D.; X. P. and H. L. performed uptake and mode of inhibition studies at OCTs under the supervision of D. H. S. All co-authors contributed to the preparation of the manuscript.

Notes

The authors declare no competing financial interest.

ACKNOWLEDGEMENTS

We thank Prof. Richard A. Glennon for fruitful discussions and proofreading the manuscript. Kavita A. Iyer was the recipient of a Lowenthal Award (2013-2015) as was Hebing Liu (2015-2017). This work was supported by the VCU Presidential Research Quest Fund (MD and DHS).

REFERENCES

1. Zhu H-J, Appel DI, Gründemann D, Richelson E, Markowitz JS. Evaluation of Organic Cation Transporter 3 (SLC22A3) Inhibition as a Potential Mechanism of Antidepressant Action. *Pharmacol. Res.* 2012; 65:491-496.

2. Nies AT, Koepsell H, Damme K, Schwab M. Organic Cation Transporters (OCTs, MATEs), *In Vitro* and *In Vivo* Evidence for the Importance of Drug Therapy. *Handb. Exp. Pharmacol.* 2010, 201;105-167.

3. Sweet DH. Renal Organic Cation and Anion Transport: From Physiology to Genes. In *Comprehensive Toxicology*; McQueen, C. A. Ed.; Academic Press: Oxford, 2010; pp 23-53.

4. Roth M, Obaidat A, Hagenbuch B. OATPs, OATs and OCTs: The Organic Anion and Cation Transporters of the SLCO and SLC22A Gene Superfamilies. *Br. J. Pharmacol.* 2012, 165;1260-1287.

5. Wu X, Kekuda R, Huang W, Fei Y-J, Leibach FH, Chen J, Conway SJ, Ganapathy V. Identity of the Organic Cation Transporter OCT3 as the Extraneuronal Monoamine Transporter ($Uptake_2$) and the Evidence for the Expression of the Transporter in the Brain. *J. Biol. Chem.* 1998, 273;32776-32786.

6. Hediger MA, Clemencon B, Burrier RE, Bruford EA. The ABCs of Membrane Transporters in Health and Disease (SLC series): Introduction. *Mol. Aspects Med.* 2013, 34;95-107.

7. Farthing CA, Sweet DH. Expression and Function of Organic Cation and Anion Transporters (SLC22 Family) in the CNS. *Curr. Pharm. Des.* 2014, 20;1472-1486.

8. Gorboulev V, Ulzheimer JC, Akhoundova A, Ulzheimer-Tueber I, Karbach U, Quester S, Baumann C, Lang F, Busch AE, Koepsell H. Cloning and Characterization of Two Human Polyspecific Organic Cation Transporters. *DNA Cell Biol.* 1997, 16;871-881.

9. Busch AE, Karbach U, Miska D, Gorboulev V, Akhoundova A, Volk C, Arndt P, Ulzheimer JC, Sonders MS, Baumann C, Waldegger S, Lang F, Koepsell H. Human Neurons Express the Polyspecific Cation Transporter hOCT2, which Translocates Monoamine Neurotransmitters, Amantadine and Memantine. *Mol. Pharmacol.* 1998, 54;342-352.

10. Koepsell H, Lips K, Volk C. Polyspecific Organic Cation Transporters: Structure, Function, Physiological Roles, and Biopharmaceutical Implications. *Pharm. Res.* 2007, 24;1227-1251.

11. Verhaagh S, Schweifer N, Barlow DP, Zwart R. Cloning of the Mouse and Human Solute Carrier 22a3 (Slc22a3/SLC22A3) Identifies a Conserved Cluster of Three Organic Cation Transporters on Mouse Chromosome 17 and Human 6q26-q27. *Genomics* 1999, 55;209-218.

12. Nies AT, Koepsell H, Winter S, Burk O, Klein K, Kerb R, Zanger UM, Keppler D, Schwab M, Schaeffeler E. Expression of Organic Cation Transporters OCT1 (SLC22A1) and OCT3 (SLC22A3) is Affected by Genetic Factors and Cholestasis in Human Liver. *Hepatology* 2009, 50;1227-1240.

13. Inyushin M, Kucheryavykh Y, Kucheryavykh L, Sanabria P, Jimenez-Rivera C, Struganova I, Eaton M, Skatchkov S. Membrane Potential and pH-Dependent Accumulation of Decynium-22 (1,1'-diethyl-2,2'-cyanine iodide) Fluorescence Through OCT Transporters in Astrocytes. *Bol. Asoc. Med. P. R.* 2010, 102;5-12.

14. Couroussé T, Gautron S. Role of Organic Cation Transporters (OCTs) in the Brain. *Pharmacol. Ther.* 2015, 146;94-103.

15. Nies AT, Koepsell H, Damme K, Schwab M. Organic Cation Transporters (OCTs, MATEs), In Vitro and In Vivo Evidence for the Importance in Drug Therapy. In *Drug Transporters*; Fromm MF, Kim RB, Eds.; Spring-Verlag: Berlin Heidelberg, 2011; pp105-167.

16. Suzuki N, Yamashita H. Novel Compound, Organic Cation Transporter 3 Detection Agent, and Organic Cation Transporter 3 Activity Inhibitor. European Patent EP3018125 A1 / WO2015002150 A1, May 11, 2016.

17. Hu T, Wang L, Pan X, Qi H. Novel Compound, Organic Cation Transporter 3 Detection Agent and Organic Cation Transporter 3 Activity Inhibitor, WO2015002150 A1: A Patent Evaluation. *Expert Opin. Ther. Pat*. 2016, 26;857-860.

18. Dukat M, Pan X, Argade M, Iyer KA, Mosier PD, Sweet DH. Dihydroquinazolines: A Novel Class of hOCT3 Inhibitors. Presented at the 249th National Meeting of the American Chemical Society, Denver, CO, March 2015; paper 264.

19. Dukat M, Abdel-Rahman AA, Ismaiel AM, Ingher S, Teitler M, Gyermek L, Glennon RA. Structure-Activity Relationships for the Binding of Arylpiperazines and Arylbiguanides at 5-HT_3 Serotonin Receptors. *J. Med. Chem.* 1996, 39;4017-4026.

20. Dukat M, Choi Y, Teitler M, Du Pre A, Herrick-Davis K, Smith C, Glennon RA. The Binding of Arylguanidines at 5-HT_3 Serotonin Receptors: A Structure-Affinity Investigation. *Bioorg. Med. Chem. Lett.* 2001, 11;1599-1603.

21. Glennon RA, Daoud MK, Dukat M, Teitler M, Herrick-Davis K, Purohit A, Syed H. Arylguanidine and Arylbiguanide Binding at 5-HT_3 Serotonin Receptors: A QSAR Study. *Bioorg. Med. Chem.* 2003, 11;4449-4454.

22. Mulgaonkar A, Venitz J, Grundemann D, Sweet DH. Human Organic Cation Transporters 1 (*SLC22A1*), 2 (*SLC22A2*), and 3 (*SLC22A3*) as Disposition Pathways for Fluoroquinolone Antimicrobials. *Antimicrob. Agents Chemother.* 2013, 57;2705-2711.

23. Pan X, Wang L, Grundemann D, Sweet DH. Interaction of Ethambutol with Human Organic Cation Transporters (SLC22 Family) Indicates Potential for Drug-Drug Interactions During Antituberculosis Therapy. *Antimicrob. Agents Chemother.* 2013, 57;5053-5059.

24. Hansch C, Leo A, Unger SH, Kim KH, Nikaitani D, Lien EJ. "Aromatic" Substituent Constants for Structure-Activity Correlations. *J. Med. Chem.* 1973, 16;1207-1216.

25. Pedersen BP, Kumar H, Waight AB, Risenmay AJ, Roe-Zurz Z, Chau BH, Schlessinger A, Bonomi M, Harries W, Sali A, Johri AK, Stroud RM. Crystal Structure of a Eukaryotic Phosphate Transporter. *Nature* 2013, 496;533-536.

26. Pao SS, Paulsen IT, Saier MH Jr. Major Facilitator Superfamily. *Microbiol. Mol. Biol. Rev.* 1998, 62;1-34.

27. Hediger MA, Romero MF, Peng J-B, Rolfs A, Takanaga H, Bruford EA. The ABCs of Solute Carriers: Physiological, Pathological and Therapeutic Implications of Human Membrane Transport Proteins. *Pflugers Arch.* 2004, 447;465-468.

28. Fredriksson R, Nordstrom KJV, Stephansson O, Hagglund MGA, Schioth HB. The Solute Carrier (SLC) Complement of the Human Genome: Phylogenetic Classification Reveals Four Major Families. *FEBS Lett.* 2008, 582;3811-3816.

29. Schlessinger A, Matsson P, Shima JE, Pieper U, Yee SW, Kelly L, Apeltsin L, Stroud RM, Ferrin TE, Giacomini KM, Sali A. Comparison of Human Solute Carriers. *Protein Sci.* 2010, 19;412-428.

30. Schlessinger A, Yee SW, Sali A, Giacomini K. M. SLC classification: An update. *Clin. Pharmacol. Ther.* 2013, 94;19-23.

31. Dakal TC, Kumar R, Ramotar D. Structural modeling of human organic cation transporters. *Comput. Biol. Chem.* 2017, 68;153-163.

32. www.rcsb.org/pdb/explore.do?structureId=5c65 accessed on June 8th, 2017.

33. Popp C, Gorboulev V, Muller TD, Gorbunov D, Shatskaya N, Koepsell H. Amino Acids Critical for Substrate Affinity of Rat Organic Cation Transporter 1 Line the Substrate Binding Region in a Model Derived from the Tertiary Structure of Lactose Permease. *Mol. Pharmacol.* 2005, 67;1600-1611.

34. Gorboulev V, Volk C, Arndt P, Akhoundova A, Koepsell H. Selectivity of the Polyspecific Cation Transporter rOCT1 is Changed by Mutation of Aspartate 475 to Glutamate. *Mol. Pharmacol.* 1999, 56;1254-1261.

35. Kellogg GE, Abraham DJ. Hydrophobicity: Is LogPo/w More Than the Sum of its Parts? *Eur. J. Med. Chem.* 2000, 35;651-661.

Figure Legends

Figure 1. Inhibitory potency determination. Representative experiments showing 1 min uptake of MPP^+ (1 μM) measured in HEK293 cells stably expressing hOCTs in the presence of increasing concentrations of phenylguanidine analogs (10^{-8} to $10^{-2.5}$ M). Data were corrected for nonspecific background measured in empty vector control cells and are shown as mean ± SD. IC_{50} values were determined with nonlinear regression and are reported in Table 1.

Figure 2. Competitive inhibition of hOCT3-mediated phenylguanidine transport. One minute cellular accumulation assays were conducted for MPP^+ (1-150 μM) in the presence and absence of two concentrations of either 4-CPG (**3**) or 4-*t*BuPG (**5**) as indicated. After correction for non-hOCT3 mediated background accumulation of MPP^+ in non-transporter expressing control cells, saturation curves were generated and analyzed by nonlinear regression to determine the mode of inhibition. Lineweaver-Burk transformations of the data are shown to readily allow visualization of the mode of inhibition as competitive.

Figure 3. Docking mode 1 of phenylguanidines with 4-*t*BuPG (**5**; white) and 4-BnPG (**6**; raspberry) superimposed at the binding region of hOCT3. The amino acid residues of hOCT3 are displayed as pale cyan lines. Dashed red lines represent ionic salt bridge interactions between the N atoms of the guanidine moiety of 4-*t*BuPG (**5**; white) and the carboxylate oxygen of Asp478 (pale cyan-capped sticks). The 4-BnPG analog is flipped over so that the guanidine moiety is pointing towards Glu451 present on the other end of the binding region

Figure 4. Docking mode 2 of 4-*t*BuPG (**5**; white) and 4-BnPG (**6**; raspberry) superimposed at the binding region of hOCT3. The amino acid residues of hOCT3 are displayed as wheat lines. Dashed red lines represent bidentate ionic salt bridge interactions between the N atoms of the guanidine moiety of phenylguanidines and the carboxylate oxygen of Asp478 (wheat-capped sticks). The 4-BnPG (**6**) analog is aligned with other phenylguanidne analogs with the guanidine moiety pointing towards Asp478. HINT analysis shows clashes between the benzyl group (meshed surface) of 4-BnPG (**6**) and Glu451 (dotted surface) present on the other end of the binding region.

TOC Graphical Abstract